Narrow-band photodetection based on *M*-plane GaN films

Sandip Ghosh , C. Rivera , J. L. Pau , E. Muñoz , O. Brandt[3], and H. T. Grahn

Department of Condensed Matter Physics and Material Science, Tata Institute of Fundamental Research, Mumbai 400005, India
ISOM and Departamento de Ingeniería Electrónica, ETSI Telecomunicación, Universidad Politécnica de Madrid, 28040 Madrid, Spain
Paul-Drude-Institut für Festkörperelektronik, Hausvogteiplatz 5–7, 10117 Berlin, Germany

Rapid identification of a range of hazardous airborne biological and chemical agents requires simultaneous detection at several specific wavelengths, and consequently a set of photodetectors with very narrow-band spectral responsivity. We demonstrate two ultraviolet photodetection configurations based on strained *M*-plane GaN films on $\mathrm{LiAlO_2}(100)$ substrates grown by molecular-beam epitaxy with a detection bandwidth below 8 nm. The optical band gap of the film depends on the orientation of the linear polarization of the incident light relative to the *c*-axis of GaN, which lies in the film plane. The first configuration consists of a polarization-sensitive planar Schottky photodetector and a filter. An orthogonal alignment of the *c*-axis of the photodetector and the filter produces a detection system with a peak responsivity at 360 nm and a bandwidth of 6 nm. The second one consists of two planar Schottky photodetectors with their *c*-axes oriented perpendicular to each other. The difference signal between the two photodetectors produces a peak responsivity at 358 nm and a bandwidth of 7.3 nm.

1 Introduction Group-III nitride semiconductors of the wurtzite crystal structure are increasingly used as ultraviolet (UV) photodetectors for applications such as solar blind detection, UV radiation dosimetry, combustion control, flame sensors, atmospheric ozone and pollution detection, data storage, and polarization-sensitive detection

In the area of biophotonics, the suitability of group-III nitride-based devices is being studied for real-time, laser-induced fluroscence detection of hazardous airborne biological and chemical agents . For a rapid identification of a range of such chemical species, it is necessary to be able to simultaneously detect radiation emitted at specific wavelengths. This requires a set of photodetectors with very narrow-band spectral responsivity. The use of band-pass interference filters exhibiting a high quality factor in combination with a broad-band detector is not ideal because of the usually poor UV transmission of typical dielectric coatings. The most common way to fabricate semiconductor UV photodetectors that operate only within a limited wavelength range is to integrate a passive filter layer into the device structure during growth. The filter layer has a larger band gap than the active region and absorbs the short-wavelength radiation, thereby limiting the short-wavelength responsivity, while the long-wavelength limit is determined by the band gap of the active region. For example, combinations consisting of $\mathrm{Al}_{x_1}\mathrm{Ga}_{1-x_1}\mathrm{N}$ as the active region and $\mathrm{Al}_{x_2}\mathrm{Ga}_{1-x_2}\mathrm{N}$ as the filter ($x_2 > x_1$) have been demonstrated with bandwidths ranging from 55 nm to 30 nm . To achieve a bandwidth of 6–7 nm in the vicinity of 360 nm, this procedure would require very precisely controlled growth of layers with $x_1 = 0$ and $x_2 = 0.03$.

We take a different approach to achieve narrow-band photodetection, which is based on GaN films of non-polar orientation such as *M*-plane or *A*-plane films [cf. inset in Fig. 1(a)]. The optical band gap of a $[1\bar{1}00]$-oriented film depends on the orientation of the in-plane polarization vector (perpendicular or parallel) with respect to the *c*-axis of GaN, which lies in the film plane. Using either a single photodetector together with a filter whose *c*-axis is

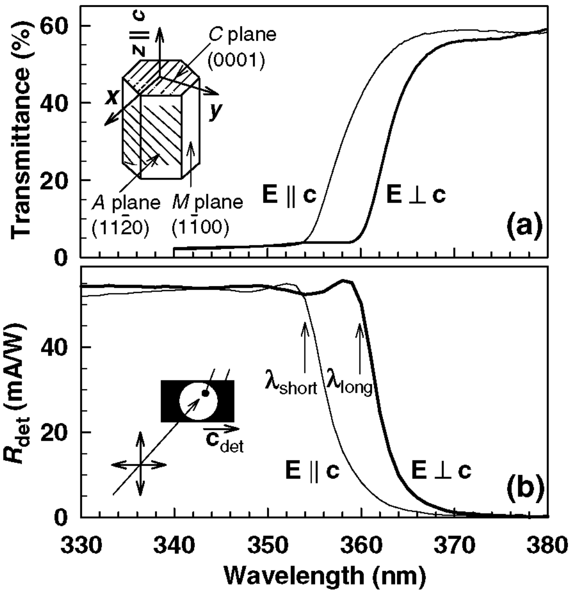

Figure 1 (a) Transmittance spectrum of sample I for $\boldsymbol{E} \perp \boldsymbol{c}$ and $\boldsymbol{E} \parallel \boldsymbol{c}$ at 297 K. The inset shows the unit cell of wurtzite GaN and the choice of coordinates. (b) Spectral responsivity R_{det} of a Schottky photodiode processed from the *M*-plane film for $\boldsymbol{E} \perp \boldsymbol{c}$ and $\boldsymbol{E} \parallel \boldsymbol{c}$. The inset depicts a schematic of the device and the measurement geometry.

oriented perpendicular to the one of the detector, or two photodetectors with their *c*-axis oriented perpendicular to each other [13], photodetection in a narrow-band detection configuration (NDBC) can be achieved.

2 Experimental details Two *M*-plane GaN films with nominal thicknesses of 400 nm were grown by rf plasma-assisted molecular-beam epitaxy on γ-LiAlO$_2$(100) substrates [14]. Their orientation and single-phase nature was verified using high-resolution X-ray diffraction (HRXRD) measurements. The out-of-plane strain ε_{yy} can also be determined by HRXRD. Both films are under an overall compressive in-plane strain with an out-of-plane dilation of $\varepsilon_{yy} = 0.39\%$ for sample I and $\varepsilon_{yy} = 0.43\%$ for sample II. The difference in the out-of-plane strain may originate from a small difference in the actual film thicknesses. The in-plane strain is anisotropic, i.e. $\varepsilon_{xx} \neq \varepsilon_{zz}$. It is mainly determined by the lattice mismatch between the film and substrate. By changing the film thickness, the in-plane strain can be varied within a certain range. Planar Schottky barrier photodetectors of circular geometry were fabricated from the wafers. For sample I, the polarization filter was taken from another piece of the same wafer. The active region of the photodetectors with a radius of 200 μm has a semitransparent, rectifying Au (12 nm thick) contact with a surrounding Ohmic contact of Ti (50 nm)/Al (200 nm) The transmittance and photocurrent spectra were obtained using light from a 75 W or 150 W Xe lamp filtered by a monochromator. The incident light beam was polarized using Glan–Taylor polarizers. The responsivity, which corresponds to the ratio of the photocurrent to the optical input for a given wavelength, was calibrated by comparison with a standard UV-enhanced Si photodiode.

3 Narrow-band detection configurations

3.1 One detector plus one filter Figure 1(a) shows the transmittance spectrum of sample I for normally incident light with the electric field vector $\boldsymbol{E}$ being polarized perpendicular ($\boldsymbol{E} \perp \boldsymbol{c}$) and parallel ($\boldsymbol{E} \parallel \boldsymbol{c}$) to the *c*-axis. The shift in the transmittance edge is due to the difference in the optical band gap for the two polarizations. This in turn leads to a polarization-dependent spectral shift in the responsivity (R_{det}) of the Schottky barrier photodetector fabricated from this film as shown in Fig. 1(b). The wavelength λ_{long} (λ_{short}) corresponds to the effective excitonic band gap for $\boldsymbol{E} \perp \boldsymbol{c}$ ($\boldsymbol{E} \parallel \boldsymbol{c}$). Note that the responsivity remains high at shorter wavelengths.

Figure 2 demonstrates that an orthogonal alignment of the *c*-axis of the photodetector ($\boldsymbol{c}_{\text{det}}$) and the filter ($\boldsymbol{c}_{\text{filt}}$) based on sample I produces a narrow-band detection configuration with a maximum value of 23 mA/W at 360 nm of the NBDC responsivity R_{NDBC} and a polarization-sensitive bandwidth at half-maximum responsivity (PSBW) of 6 nm. This combination of detector and filter works as follows. In this GaN film, the band gap (λ_{long} or λ_{short}) depends on the polarization state of the incoming light beam ($\boldsymbol{E} \perp \boldsymbol{c}_{\text{det}}$ or $\boldsymbol{E} \parallel \boldsymbol{c}_{\text{det}}$, respectively). For $\boldsymbol{E} \perp \boldsymbol{c}_{\text{det}}$, light with $\lambda \leq \lambda_{\text{short}}$ is absorbed by the filter and consequently prevented from reaching the detector, while light with $\lambda_{\text{short}} \leq \lambda \leq \lambda_{\text{long}}$ is transmitted by the filter and can therefore reach the detector. In contrast, all light with $\lambda \leq \lambda_{\text{long}}$ will be absorbed by the filter for $\boldsymbol{E} \parallel \boldsymbol{c}_{\text{det}}$ so that no light of this polarization reaches the detector. The presence of the small signal for $\boldsymbol{E} \parallel \boldsymbol{c}_{\text{det}}$ is essentially due to absorption at energies below the band gap. The measured dependence of R_{NBDC} at 360 nm on the in-plane polarization angle ϕ, which is defined relative to $\boldsymbol{c}_{\text{det}}$, follows the ex-

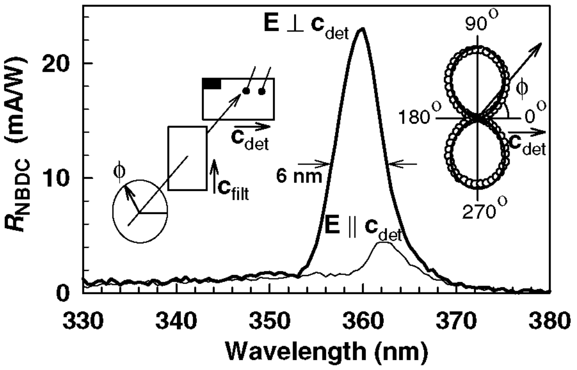

Figure 2 Spectral responsivity R_{NBDC} of the NBDC based on sample I for $\boldsymbol{E} \perp \boldsymbol{c}_{\text{det}}$ and $\boldsymbol{E} \parallel \boldsymbol{c}_{\text{det}}$ at 297 K. The left inset displays the measurement configuration. The right inset depicts a polar plot of the measured relative R_{NBDC} at 360 nm (circles) as a function of the in-plane polarization angle ϕ, the line represents a fit to $R_{\text{NBDC}} = R^{\max} \sin^2(\phi)$.

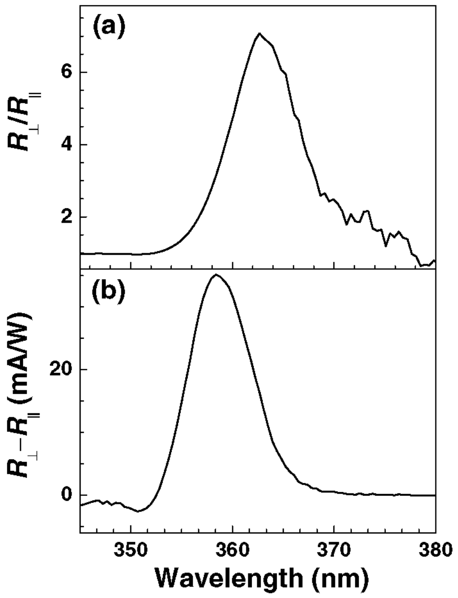

Figure 3 (a) Contrast of the responsivities $R_\perp/R_\parallel$ in sample II for polarization perpendicular ($R_\perp$) and parallel ($R_\parallel$) to the c-axis at room temperature. (b) $R_\perp - R_\parallel$ response for sample II at room temperature.

pected relation $R_{\mathrm{NBDC}} = R^{\max}\sin^2(\phi)$ (cf. the right inset in Fig. 2).

3.2 Two detectors Figure 3(a) shows the measured contrast $R_\perp/R_\parallel$ for sample II. The $R_\perp/R_\parallel$ contrast and the PSBW determined from Fig. 3(a) are 7.25 at 363 nm and 7.7 nm, respectively. These values demonstrate the feasibility of using this type of photodetectors in practical applications. The polarization sensitivity, restricted to the vicinity of the energy gap, could be shifted to shorter or longer wavelengths using (Al,Ga,In)N films. In order to increase the intrinsic $R_\perp/R_\parallel$ contrast, a detection scheme for $R_\perp - R_\parallel$ is proposed. In this scheme, the signal must be detected simultaneously by two devices, which are placed side by side, with their c-axes oriented in orthogonal directions so that the difference can be further amplified. As shown in Fig. 3(b), the peak contrast of $R_\perp - R_\parallel$ shifts to higher energies with a peak responsivity and PSBW of 35 mA/W at 358 nm and 7.3 nm, respectively. The sign of the detected signal determines the polarization state of the incident light, i. e., either perpendicular or parallel to the c-axis. The rejection ratio for wavelengths outside of the detection band is larger than 100 so that narrow-band detection is additionally achieved.

For both types of NBDC, one could also use A-plane GaN films grown on R-plane sapphire or A-plane SiC

However, for the detector-filter configuration, only the substrates $LiAlO_2$ and sapphire are transparent down to 200 nm and can therefore be used in the UV spectral range. Furthermore, in terms of the necessary in-plane strain values, only M-plane GaN films on $LiAlO_2$ can experience large anisotropic strain values. Finally, since both types of NBDC are additionally polarization sensitive, they may also reduce spurious background signals.

4 Conclusions We have proposed and demonstrated very narrow-band photodetection in the UV spectral range using wurtzite group-III nitride films of non-polar orientation, which in addition to its narrow-band spectral responsivity is also polarization sensitive. The anisotropic in-plane strain, which is naturally present in such films, is essential for the efficient operation of such detection systems. We have presented two configurations consisting of either a single detector and a filter or two detectors with their c-axes oriented perpendicular to each other. These configurations, when used specifically for polarization sensing, may also perform better than a single polarization-sensitive photodetector, because the limited spectral bandwidth ensures a lower spurious background signal.

References

M. Razeghi and A. Rogalski, J. Appl. Phys. **79**, 7433 (1996).

G. Parish, S. Keller, P. Kozodoy, J. P. Ibbetson, H. Marchand, P. T. Fini, S. B. Fleischer, S. P. DenBaars, U. K. Mishra, and E. J. Tarsa, Appl. Phys. Lett. **75**, 247 (1999).

E. Muñoz, E. Monroy, F. Calle, F. Omnès, and P. Gibart, J. Geophys. Res. **105**, 4865 (2000).

J. L. Pau, J. Anduaga, C. Rivera, Á. Navarro, I. Álava, M. Redondo, and E. Muñoz, Appl. Opt. **45**, 7498 (2006).

T. Li, J. H. Lambert, A. L. Beck, C. J. Collins, B. Yang, M. M. Wong, U. Chowdhury, R. D. Dupuis, and J. C. Campbell, J. Electron. Mater. **30**, 872 (2001).

M. A. Khan, M. Shatalov, H. P. Maruska, H. M. Wang, and E. Kuokstis, Jpn. J. Appl. Phys. **44**(1), 7191 (2005).

S. Ghosh, O. Brandt, H. T. Grahn, and K. H. Ploog, Appl. Phys. Lett. **81**, 3380 (2002).

C. Rivera, J. L. Pau, E. Muñoz, P. Misra, O. Brandt, H. T. Grahn, and K. H. Ploog, Appl. Phys. Lett. **88**, 213507 (2006).

G. A. Wilson and R. K. DeFreez, Proc. SPIE **5416**, 157 (2004).

S. K. Zhang, W. B. Wang, F. Yun, L. He, H. Morkoç, X. Zhou, M. Tamargo, and R. R. Alfano, Appl. Phys. Lett. **81**, 4628 (2002).

U. Karrer, A. Dobner, O. Ambacher, and M. Stutzmann, J. Vac. Sci. Technol. B **18**, 757 (2000).

S. Ghosh, C. Rivera, J. L. Pau, E. Muñoz, O. Brandt, and H. T. Grahn, Appl. Phys. Lett. **90**, 091110 (2007).

C. Rivera, P. Misra, J. L. Pau, E. Muñoz, O. Brandt, H. T. Grahn, and K. H. Ploog, Proceedings of the 6th Spanish Conference on Electronic Devices, San Lorenzo de El Escorial, Madrid, Spain (IEEE, Piscataway, 2007), pp. 250–253.

P. Waltereit, O. Brandt, M. Ramsteiner, R. Uecker, P. Reiche, and K. H. Ploog, J. Cryst. Growth **218**, 143 (2000).

S. Ghosh, P. Misra, H. T. Grahn, B. Imer, S. Nakamura, S. P. DenBaars, and J. S. Speck, J. Appl. Phys. **98**, 026105 (2005).

P. Misra, U. Behn, O. Brandt, H. T. Grahn, B. Imer, S. Nakamura, S. P. DenBaars, and J. S. Speck, Appl. Phys. Lett. **88**, 161920 (2006).